

---

# A numerical study of thermal convection in a rotating spherical annulus with axial gravitational field by using parametric spline function approximation

Numerical study  
of thermal  
convection

673

Received September  
1995  
Revised September  
1996

C.V. Raghavarao and S.T.P.T. Srinivas

*Department of Mathematics, Indian Institute of Technology, Madras,  
India*

## 1. Introduction

Combined convection in rotating spherical annuli is of great interest in both engineering design and geophysics. The problem can be divided into two cases. The first is the case in which the gravitational field acts in radial direction and the second is that in which the gravitational field acts in the direction parallel to that of the axis of rotation. Although seemingly a minor change, the two problems are entirely different except in the forced convection limit. The former model is applicable to some geophysical or meteorological situations. The latter model is applicable to such physical flows as a rotating sphere viscometer (Bestman, 1978).

In the past several studies concerning both cases were carried out. Pedlosky (1969) studied the steady motion of a thermally stratified fluid in a narrow spherical annulus with radial gravitational field. Douglass *et al.* (1978) obtained an approximate solution for the same problem using a modified Galerkin technique for moderate Reynolds numbers and several angular velocity ratios. The effects of different ratios of radii spheres on combined convection are shown in Douglass *et al.* (1979) in which a fourth order regular perturbation expansion method in powers of Reynolds number is used to solve the governing equations. A numerical investigation is performed by Raghavarao and Srinivas (1995a) for a similar problem using a parametric spline function approximation to solve the governing Navier Stokes and energy equations.

An early study of combined convection flows in concentric spherical annulus with the gravitational field in axial direction is that of Riley and Mack (1972). They used a lower order perturbation expansion in powers of Reynolds number to obtain the approximate solution to the governing equations. Maples *et al.* (1973) studied the combined convection in spherical annulus experimentally. In their study only the inner sphere is allowed to rotate and Nusselt number

International Journal of Numerical  
Methods for Heat & Fluid Flow  
Vol. 8 No. 6, 1998, pp. 673–688.  
© MCB University Press, 0961-5539

dependence on Grashof and Reynolds numbers is presented graphically. Reynolds numbers ranged upward from 3,000. Another analytical study is by Dallman and Douglass (1980) in which a partial spectral expansion method is used to solve the governing equations.

The details of the spline function approximation and its applications to convective flows can be found in Lauriat and Altimir (1985), Wang (1987) and Wang *et al.* (1990). In Lauriat and Altimir (1985), spline alternating direction implicit (SADI) method and in Wang (1987) and Wang *et al.* (1990) spline method of fractional steps (SMFS) was used to solve the governing equations. Both the methods depend on cubic spline. The parametric spline function approximation was earlier used by Jain and Aziz (1981) to solve ordinary and partial differential equations occurring in applied mechanics. Raghavarao and Srinivas (1995b) applied this technique to obtain the approximate solutions for the inviscid flow past a circular cylinder and Stokes' flow past a sphere. Later, it is applied to obtain the approximate solution for thermal convection in rotating concentric spherical annulus with a uniform radial gravitational field (Raghavarao and Srinivas, 1995a).

The present study is devoted to a numerical investigation of the combined convection of the flow between two concentric rotating spheres with axial gravitational field using a parametric spline function approximation. The advantage of spline function approximation over usual finite difference scheme (FDS) is in FDS the non-linear terms in the governing equations are approximated by the upwind difference scheme which is of first order accuracy, whereas, in spline function approximation the first order derivatives in the non-linear terms are eliminated by second order derivatives whose values are calculated. Both the elimination of first order derivatives and calculation of values of second order derivatives is done by using suitable spline relations and the approximation gives second order accuracy. The computations are done for different values of Reynolds number, Prandtl number and angular velocity ratios.

## 2. Governing equations

Here the steady combined thermal convection of a viscous Boussinesq fluid contained between two concentric spheres is considered. The spheres are considered to be at different temperatures and are in rotation with different angular velocities about a common vertical axis. A uniform gravitational field acts on the fluid in the direction parallel to the axis of rotation. The system of equations describing the flow field for the combined convection situation are the dimensionless Navier-Stokes' equations and the energy equation. These equations in terms of the stream function in the meridian plane  $\psi$ , an angular momentum function  $\Omega$ , and temperature  $T$  are as follows:

$$\frac{1}{Re} D^2\Omega = \frac{1}{r^2 \sin \theta} \frac{\partial(\Omega, \psi)}{\partial(r, \theta)}, \quad (1)$$

$$\frac{1}{Re} D^4 \psi = -\frac{Gr}{Re^2} \sin \theta \frac{\partial(r \cos \theta, T)}{\partial(r, \theta)} + \frac{1}{r^2 \sin \theta} \left\{ \frac{2}{r \sin \theta} \left[ \Omega \frac{\partial(-r \sin \theta, \Omega)}{\partial(r, \theta)} + D^2 \psi \frac{\partial(-r \sin \theta, \psi)}{\partial(r, \theta)} \right] + \frac{\partial(D^2 \psi, \psi)}{\partial(r, \theta)} \right\} \quad (2)$$

$$\nabla^2 T = \frac{Re Pr}{r^2 \sin \theta} \frac{\partial(T, \psi)}{\partial(r, \theta)}, \quad (3)$$

where

$$D^2 = \frac{\partial^2}{\partial r^2} - \frac{\cot \theta}{r^2} \frac{\partial}{\partial \theta} + \frac{1}{r^2} \frac{\partial^2}{\partial \theta^2}, D^4 = D^2(D^2)$$

and  $\nabla^2$  is the Laplacian operator in spherical polar coordinates.

The dimensionless parameters are defined as  $Re = \omega_0 R_2^2/\nu$ ,  $Gr = g_0 \beta (T_2 - T_1) R_2^3/\nu$  and  $Pr = \nu/\alpha$ .

Equation (2) can be split into two coupled equations as:

$$D^2 \psi = \zeta = \zeta_1 \sin \theta, \quad (4)$$

$$\frac{1}{Re} D^2 \zeta = -\frac{Gr}{Re^2} \sin \theta \frac{\partial(r \cos \theta, T)}{\partial(r, \theta)} + \frac{1}{r^2 \sin \theta} \left\{ \frac{2}{r \sin \theta} \left[ \Omega \frac{\partial(-r \sin \theta, \Omega)}{\partial(r, \theta)} + \zeta \frac{\partial(-r \sin \theta, \psi)}{\partial(r, \theta)} \right] + \frac{\partial(\zeta, \psi)}{\partial(r, \theta)} \right\} \quad (5)$$

In equation (4),  $\zeta_1$  is the vorticity. The solutions have only axisymmetry and the ranges of independent variables are  $\eta \leq r \leq 1$  and  $0 \leq \theta \leq \pi$ . Here  $\eta = R_1/R_2$ , where  $R_1$  and  $R_2$  are the radii of the inner and outer spheres respectively.

The boundary conditions which complete the formulation of the problem are as follows:

$$\psi = \frac{\partial \psi}{\partial r} = 0 \text{ on } r = \eta, 1$$

HFF  
8,6

$$T = 0 \text{ on } r = \eta \text{ and } T = 1 \text{ on } r = 1$$

$$\Omega = \frac{\eta^2}{\bar{\mu}} \sin^2 \theta \text{ on } r = \eta \text{ and } \Omega = \sin^2 \theta \text{ on } r = 1,$$

**676**

where  $\bar{\mu} = \omega_2/\omega_1$ ,  $\omega_1$  and  $\omega_2$  are the angular velocities of the inner and outer spheres respectively.

$$\text{Also } \psi = \frac{\partial \psi}{\partial \theta} = 0 \text{ and } \frac{\partial T}{\partial \theta} = 0, \text{ on } \theta = 0 \text{ and } \pi \text{ (lines of symmetry).}$$

The boundary conditions on  $\zeta$  are:

$$\zeta = \frac{8\psi_1 - \psi_2}{2h^2} \text{ on the inner sphere,}$$

$$\zeta = \frac{8\psi_{N-1} - \psi_{N-2}}{2h^2} \text{ on the outer sphere.}$$

and  $\zeta = 0$  on the lines of symmetry.

These boundary conditions on  $\zeta$  are obtained by taking a third degree polynomial approximation to  $\psi$  and using the definition of  $\zeta$  and zero velocities on the surfaces of the spheres.

### 3. Method of solution

Approximate solutions to the governing equations are obtained by parametric spline function approximation. The parametric spline function is defined as follows (Jain and Aziz, 1981).

A function  $S(t)$ , of class  $C^2(a,b)$  which interpolates  $y(t)$  at the knots  $\{t_i\}$  depends on a parameter  $\rho > 0$ , and reduces to a cubic spline in the interval  $(t_{i-1}, t_i)$  as  $\rho \rightarrow 0$ , is termed as a parametric spline function and is given by:

$$\begin{aligned} S(t) = & -\frac{h^2}{w^2 \sin w} \left[ S'''(t_i) \sin w \frac{(t - t_{i-1})}{h} + S'''(t_{i-1}) \sin w \frac{(t_i - t)}{h} \right] \\ & + \frac{h^2}{w^2} \left[ \frac{(t - t_{i-1})}{h} \left( S''(t_{i-1}) + \frac{w^2}{h^2} S(t_i) \right) \right. \\ & \left. + \frac{(t_i - t)}{h} \left( S''(t_i) + \frac{w^2}{h^2} S(t_{i-1}) \right) \right] \end{aligned} \quad (6)$$

where  $w = h\sqrt{\rho}$ .

The additional spline relations that are useful in solving the governing equations are:

$$y_{i+1} - 2y_i + y_{i-1} = h^2(\alpha M_{i+1} + 2\beta M_i + \alpha M_{i-1}), \quad (7)$$

$$m_i = -h(\alpha M_{i+1} + \beta M_i) + \frac{y_{i+1} - y_i}{h} \quad (8)$$

$$m_{i-1} = h(\alpha M_{i-1} + \beta M_i) + \frac{y_i - y_{i-1}}{h}, \quad (9)$$

where

$$S(t_i) = y_i, \quad S'(t_i) = m_i, \quad S''(t_i) = M_i, \quad \alpha = \frac{1}{w^2} \left( \frac{w}{\sin w} - 1 \right),$$

$$\text{and } \beta = \frac{1}{w^2} \left( 1 - \frac{w}{\sin w} \cos w \right)$$

Here we take the parametric spline function approximation in  $r$ -direction and finite differences (central differences) in  $\theta$ -direction. The intervals are taken as  $h = 0.02$  in  $r$ -direction and  $k = \pi/45$  in  $\theta$ -direction.  $R_1$  and  $R_2$  are taken as 0.5 and 1.0 respectively. Now equations (1), (4), (5) and (3) can be written as:

$$Q_{i,j} \left[ 1 + h\beta \frac{Re}{r_i^2 \sin \theta_j} \frac{(\psi_{i,j+1} - \psi_{i,j-1})}{2k} \right] = \frac{Re}{r_i^2 \sin \theta_j} \frac{(\psi_{i,j+1} - \psi_{i,j-1})}{2k}$$

$$\left[ -h\alpha Q_{i+1,j} + \frac{(\Omega_{i+1,j} - \Omega_{i,j})}{h} \right] + \frac{\cot \theta_j}{r_i^2} \frac{(\Omega_{i,j+1} - \Omega_{i,j-1})}{2k}$$

$$- \frac{(\Omega_{i,j+1} - 2\Omega_{i,j} + \Omega_{i,j-1})}{r_i^2 k^2} - \frac{Re}{r_i^2 \sin \theta_j} \frac{(\Omega_{i,j+1} - \Omega_{i,j-1})}{2k} \frac{(\psi_{i+1,j} - \psi_{i-1,j})}{2h} \quad (10)$$

$$P_{i,j} = \frac{\cot \theta_j}{r_i^2} \frac{(\psi_{i,j+1} - \psi_{i,j-1})}{2k} - \frac{(\psi_{i,j+1} - 2\psi_{i,j} + \psi_{i,j-1})}{r_i^2 k^2} + \zeta_{i,j} \quad (11)$$

$$R_{i,j} \left[ 1 + h\beta \frac{Re}{r_i^2 \sin \theta_j} \frac{(\psi_{i,j+1} - \psi_{i,j-1})}{2k} \right] = \frac{Re}{r_i^2 \sin \theta_j} \frac{(\psi_{i,j+1} - \psi_{i,j-1})}{2k}$$

$$\left[ -h\alpha R_{i+1,j} + \frac{(\zeta_{i+1,j} - \zeta_{i,j})}{h} \right] + \frac{\cot \theta_j}{r_i^2} \frac{(\zeta_{i,j+1} - \zeta_{i,j-1})}{r_i^2 k^2}$$

$$- \frac{Gr}{Re^2} Re \sin \theta_j \left[ \cos \theta_j \frac{(T_{i,j+1} - T_{i,j-1})}{2k} + r_i \sin \theta_j \frac{(T_{i+1,j} - T_{i-1,j})}{2h} \right]$$

$$\frac{Re}{r_i^2 \sin \theta_j} \left[ 2\Omega_{i,j} \left\{ \cot \theta_j \frac{(\Omega_{i+1,j} - \Omega_{i-1,j})}{2h} - \frac{(\Omega_{i,j+1} - \Omega_{i,j-1})}{r_i 2k} \right\} + 2\zeta_{i,j} \left\{ \cot \theta_j \frac{(\psi_{i+1,j} - \psi_{i-1,j})}{2h} - \frac{(\psi_{i,j+1} - \psi_{i,j-1})}{r_i 2k} \right\} - \frac{(\psi_{i+1,j} - \psi_{i-1,j})(\zeta_{i,j+1} - \zeta_{i,j-1})}{2h 2k} \right] \quad (12)$$

$$S_{i,j} \left[ 1 - h\beta \left\{ \frac{2}{r_i} - \frac{RePr}{r_i^2 \sin \theta_j} \frac{(\psi_{i,j+1} - \psi_{i,j-1})}{2k} \right\} \right] = \frac{-\cot \theta_j (T_{i,j+1} - T_{i,j-1})}{r_i^2} - \frac{(T_{i,j+1} - 2T_{i,j} + T_{i,j-1})}{r_i^2 k^2} - \frac{RePr}{r_i^2 \sin \theta_j} \frac{(T_{i,j+1} - T_{i,j-1})(\psi_{i+1,j} - \psi_{i-1,j})}{2k 2h} - \left[ \frac{2}{r_i} - \frac{RePr}{r_i^2 \sin \theta_j} \frac{(\psi_{i,j+1} - \psi_{i,j-1})}{2k} \right] \left[ -h\alpha S_{i+1,j} + \frac{(T_{i+1,j} - T_{i,j})}{h} \right] \quad (13)$$

where  $P_{i,j}$ ,  $Q_{i,j}$ ,  $R_{i,j}$  and  $S_{i,j}$  are the second order partial derivatives of  $\psi$ ,  $\Omega$ ,  $\zeta$  and  $T$  respectively with respect to  $r$  at the mesh point  $(r_i, \theta_j)$ . Here  $i = 1, 2, \dots, N-1, j = 1, 2, \dots, L-1$  and  $N_h = 0.5, Lk = \pi$ .

The above equations, along with the corresponding spline relations obtained from (7) are solved simultaneously with conditions for  $P$ ,  $Q$ ,  $R$  and  $S$  on the bounding surfaces derived from the governing equations using the boundary conditions for the flow parameters on the surfaces of the spheres. The expressions for  $P$ ,  $Q$ ,  $R$  and  $S$  are:

$$Q_{0,j} = \frac{\cot \theta_j (\Omega_{0,j+1} - \Omega_{0,j-1})}{R_1^2 2k} - \frac{1}{R_1^2} \frac{(\Omega_{0,j+1} - 2\Omega_{0,j} + \Omega_{0,j-1})}{k^2} \quad (14)$$

$$Q_{N,j} = \frac{\cot \theta_j (\Omega_{N,j+1} - \Omega_{N,j-1})}{R_2^2 2k} - \frac{(\Omega_{N,j+1} - 2\Omega_{N,j} + \Omega_{N,j-1})}{R_2^2} \quad (15)$$

$$P_{0,j} = \zeta_{0,j} \quad (16)$$

$$P_{N,j} = \zeta_{N,j} \quad (17)$$

$$R_{0,j} = \frac{\cot \theta_j (\zeta_{0,j+1} - \zeta_{0,j-1})}{R_1^2 2k} - \frac{(\zeta_{0,j+1} - 2\zeta_{0,j} + \zeta_{0,j-1})}{R_1^2 k^2} + \frac{Re}{R_1^2 \sin \theta_j} \left[ 2\Omega_{0,j} \left\{ \cot \theta_j \frac{(\Omega_{1,j} - \Omega_{0,j})}{h} - \frac{(\Omega_{0,j+1} - \Omega_{0,j-1})}{R_1^2 k^2} \right\} + 2\zeta_{0,j} \cot \theta_j \frac{\psi_{1,j}}{h} \right] \quad (18)$$

$$R_{N,j} = \frac{\cot \theta_j (\zeta_{N,j+1} - \zeta_{N,j-1})}{R_2^2} - \frac{(\zeta_{N,j+1} - 2\zeta_{N,j} + \zeta_{N,j-1})}{R_2^2 k^2} + \frac{Re}{R_2^2 \sin \theta_j} \left[ 2\Omega_{N,j} \left\{ \cot \theta_j \frac{(\Omega_{N,j} - \Omega_{N-1,j})}{h} - \frac{(\Omega_{N,j+1} - \Omega_{N,j-1})}{R_2^2 k^2} \right\} - 2\zeta_{N,j} \cot \theta_j \frac{\psi_{N-1,j}}{h} \right] \quad (19)$$

$$S_{0,j} = 2(h\alpha S_{1,j} - \frac{T_{1,j}}{h}) \quad (20)$$

$$S_{N,j} = \frac{-2}{(R_2 + 2h\beta)} \left[ h\alpha S_{N-1,j} + \frac{(1 - T_{N-1,j})}{h} \right] \quad (21)$$

The initial values for  $P$ ,  $Q$ ,  $R$ ,  $S$  and  $\psi$ ,  $\Omega$ ,  $\zeta$ , and  $T$  are taken as zeros. By using Gauss-Seidel method the equations (10)-(13) with conditions (14)-(21) are solved for  $Q_{i,j}$ ,  $P_{i,j}$ ,  $R_{i,j}$  and  $S_{i,j}$ . Subsequently these values are used to solve, by Gauss-Seidel method, for  $\Omega_{i,j}$ ,  $\psi_{i,j}$ ,  $\zeta_{i,j}$  and  $T_{i,j}$  using the corresponding spline relations from the equation (7).

This completes one iteration. The iterative process continued till  $|F^{(n+1)} - F^{(n)}| < 10^{-6}$ , where  $F = \psi, \Omega, \zeta, T, P, Q, R$  and  $S$ .

#### 4. Discussion of results

There are five dimensionless parameters governing the flow and heat transfer in the rotating annulus viz.  $\eta$ ,  $\bar{\mu}$ ,  $Re$ ,  $Gr/Re^2$  and  $Pr$ . Here  $\eta$  and  $\bar{\mu}$  are determined by the geometry and boundary conditions.  $Re$  and  $Gr/Re^2$  are measures of dynamical effects and  $Pr$  depends on the fluid properties. The ratio of the radii  $\eta$  is fixed as 0.5 throughout the discussion while the other parameters are varied to account for their influence on the flow. A computer program is developed to evaluate  $\psi$ ,  $\Omega$ ,  $\zeta$ , and  $T$ .

There would be no fluid motion in the annulus, if the bounding spheres are stationary and the temperature distribution is simply due to conduction. In reality there will be still motion (secondary) of the fluid due to natural convection and the temperature distribution would be due to conduction and also due to natural convection. Any rotation of the bounding spheres causes a primary flow ( $\omega$ ) around the axis of rotation, whereas the secondary flow ( $\psi$ ) has its origin in two different mechanisms. One is the centrifugal acceleration of the fluid generated by the primary flow and the other is the buoyancy force caused by the density variations due to non-uniform temperatures in the fluid. In the first extreme (i.e. given by either isothermal flow or forced convection) the flow pattern is well established as being both axially and equatorially symmetric. The other extreme of natural convection in spherical annulus has only axisymmetry. It is, therefore, reasonable that these two mechanisms together contribute to form flows with the characteristics of both extremes.

The suitable measure of the relative importance of these mechanisms is  $Gr/Re^2$ . The forced convection case is given by  $Gr/Re^2 = 0$  which uncouples the equations (2) and (3).

---

HF  
8,6

Calculations are made for:

- different values of  $Re$  viz.  $Re = 50, 100, 150$  for  $Gr/Re^2 = 1, \bar{\mu} = 2, Pr = 1$  to show the effects of  $Re$ ;
- $Re = 50, Gr/Re^2 = 1, \bar{\mu} = 2, Pr = 10$ , to show the effects of  $Pr$ ; and
- $Re = 50, Gr/Re^2 = 0, 1/10, 1/3$  and  $\bar{\mu} = -1/3, Pr = 1$  to show the effects of both  $Gr/Re^2$  and the angular velocity ratios of the spheres.

680

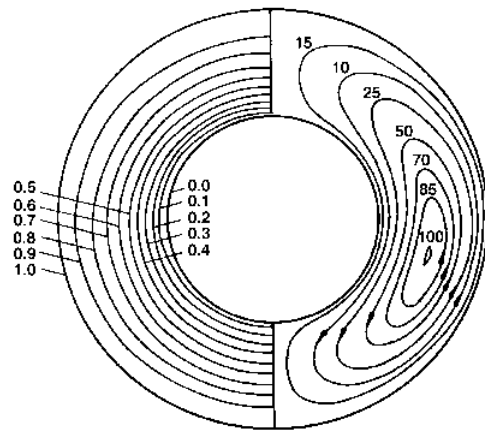
---

The first effect to be discussed is that of increasing  $Re$ . The other parameters are taken as  $Gr/Re^2 = 1, Pr = 1$  and  $\bar{\mu} = 2$ .  $\bar{\mu} = 2$  implies that both the spheres are rotating in the same direction and the outer sphere is rotating with a velocity twice that of the inner sphere. Changes in secondary flow in response to increasing  $Re$  are shown in right side of Figure 1(a) to 1(c). As it is seen the secondary flow consists of "kidney" shaped eddy and the centrifugal accelerations due to rotation in an enhanced counterclockwise circulation of the eddy. As  $Re$  increases this effect increases. The result for  $Re = 50$  is in good comparison with that of Dallman and Douglass (1980), whereas the secondary flow streamline patterns and temperature distribution results are not available for comparison for  $Re = 100, 150$ .

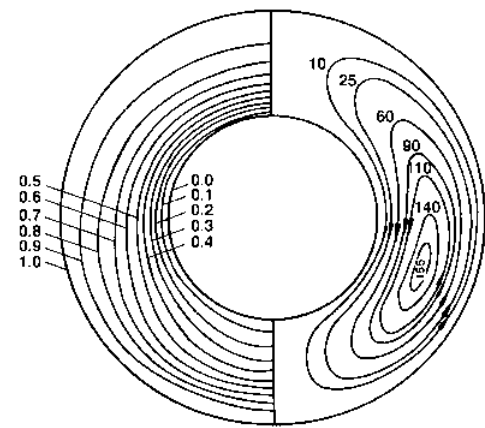
Isotherms for the same parameters are shown in Figure 1 (left side). At  $Re = 50$ , isotherms (consist of lines of constant  $T$ ) are pushed slightly towards the outer sphere in the southern hemisphere and towards the inner sphere in the northern hemisphere. This trend significantly increases as  $Re$  increases. This behavior is explained in terms of the secondary flow results as follows: as the cold fluid moves upward from its coldest point near the south pole, it is heated by the warm outer sphere. This tends to produce large thermal gradients at the outer sphere near the north pole. The fluid gets heated continuously as it moves toward the north pole. Then, in a region near the north pole, a relatively large amount of warm fluid is formed. This is reflected in the isotherms being more concentrated near the inner sphere. A cooling phenomenon similar to that for the outer sphere occurs as the warm fluid sweeps along the cool inner sphere which ultimately causes a relatively large area of cold fluid near the south pole to develop.

Distribution of angular velocity is shown in Figure 2 for the same set of parameters. Unlike for small values of  $Re$ , given in Riley and Mack (1972), when  $Re = 50$ , the contours of constant angular velocity are not concentric circles, but they are distorted and in some regions angular velocity of the fluid is higher than that of the boundaries. Although it seems to be incorrect at first sight, this behavior can be shown to be possible by referring to the isotherms of Figure 1 and conservation of angular momentum. From isotherms shown in Figure 1, it is seen that as  $Re$  increases, relatively larger regions of warm and cold fluid regions form near the north and south poles respectively as compared to the low  $Re$  results. Being more dense, the colder fluid rotates slower than the forced convection flow. On the other hand, the warm less-dense fluid must rotate faster and in some regions with more angular velocities than boundaries. It is

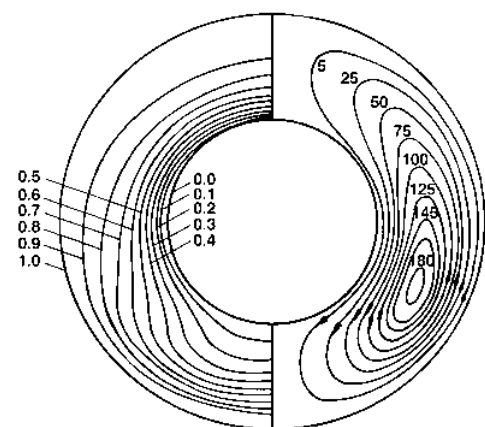




(a)



(b)



(c)

**Figure 1.**  
Isotherms and  
secondary flow ( $-10^4\psi$ )  
for  $\bar{\mu} = 2$ ,  $\eta = 0.5$ ,  
 $Gr/Re^2 = 1$ ,  $Pr = 1$ :  
(a)  $Re = 50$ ; (b)  $Re = 100$ ;  
(c)  $Re = 150$

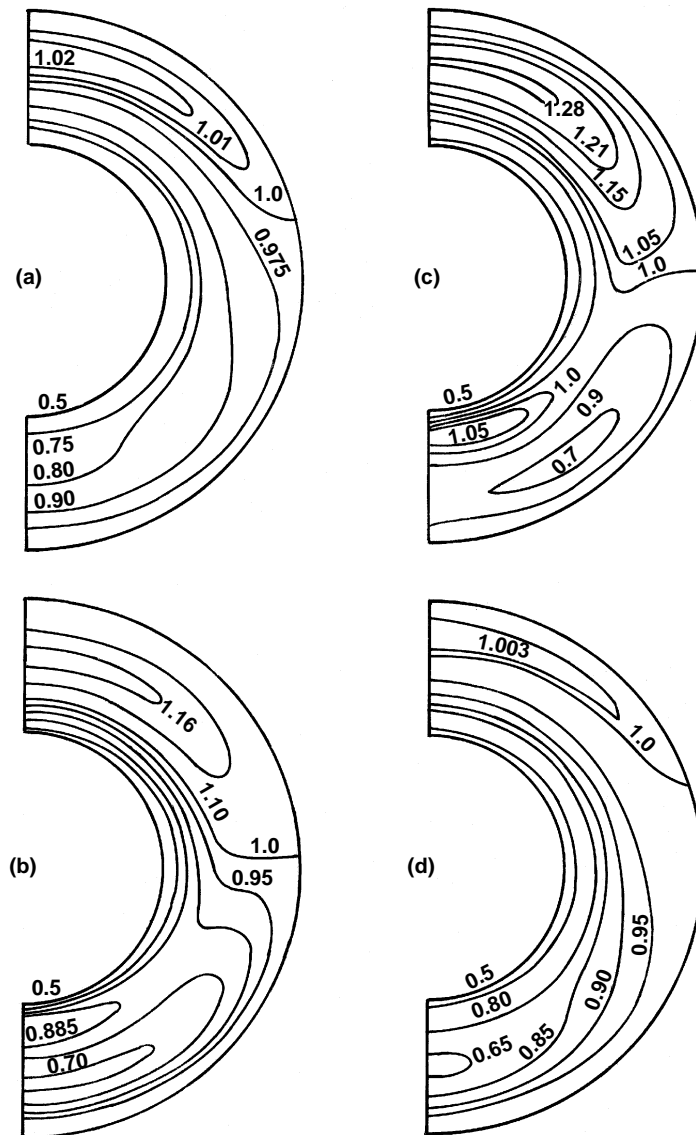


**Figure 2.**  
Angular velocity  
distributions for  $\bar{\mu} = 2$ ,  
 $\eta = 0.5$ ,  $Gr/Re^2 = 1$ ,  
 $Pr = 1$ : (a)  $Re = 50$ ;  
(b)  $Re = 100$ ; (c)  $Re = 150$ ;  
(d)  $Re = 50$  and  $Pr = 10$

observed that the warm fluid rotates at over 116 and 128 per cent of the speed of the outer sphere for  $Re = 100$  and  $150$  respectively.

The second effect to be studied is due to the Prandtl number  $Pr = \nu/\alpha$ . Since the Prandtl number depends on the fluid properties only, changing  $Pr$  means changing the working fluid. A large value of  $Pr$  means that the fluid can diffuse more momentum than energy. Thus the velocity gradients are smaller than the thermal gradients. The converse follows for small values of  $Pr$  ( $< 1$ ) and for  $Pr = 1$  both the gradients are of the same magnitude. The secondary flow

streamline pattern and temperature distribution for  $Pr = 10$  are shown in Figure 3. It is observed that for  $Pr = 10$ , a large region of the southern hemisphere is filled by very cold fluid forming a thermal boundary layer along the southern part of the warm outer sphere. A less pronounced large region of warm fluid occupies the northern inner sphere. From Figure 1(a), it is seen that for  $Pr = 1$ , these segregated regions are only slightly established. In both cases, the secondary flow causes the fluid to be swept upward along the warm outer sphere and downward along the cold inner sphere. Also, the larger  $Pr$  is more resistant to changing its temperature, causing large warm and cold regions to persist in the annulus.

The final effect is that of the ratio  $Gr/Re^2$ , which shows the relative effect of increasing gravitational forces. The calculations are made for  $\eta = 0.5$ ,  $\tilde{\mu} = -1/3$ ,  $Pr = 1$ ,  $Re = 50$ ,  $Gr/Re^2 = 0, 1/10, 1/3, 1$ .  $\tilde{\mu} = -1/3$  implies that both the spheres are rotating, the inner sphere is rotating three times faster than the outer sphere and in the opposite direction. Isotherms and secondary flow streamlines are given in Figure 4. Figure 4(a) shows the result for  $Gr/Re^2 = 0$ , i.e. the buoyancy forces are zero which is the case of forced convection. The secondary flow is driven by the centrifugal force field established by the differential rotation of the two spheres. This flow has equatorial symmetry. The shear driven secondary flow consists of two counter rotating torodial eddies. The eddy near the inner sphere has a strong counterclockwise circulation; the other eddy has a slightly weaker clockwise circulation. The differences in the strength and direction of the flow in these convective motions reflect the fact that the inner sphere is rotating three times as fast as the outer sphere and in the opposite direction. The introduction of a slight buoyancy force ( $Gr/Re^2=1/10$ , Figure 4(b)), alters the secondary flow and causes the equatorial symmetry to vanish by combining

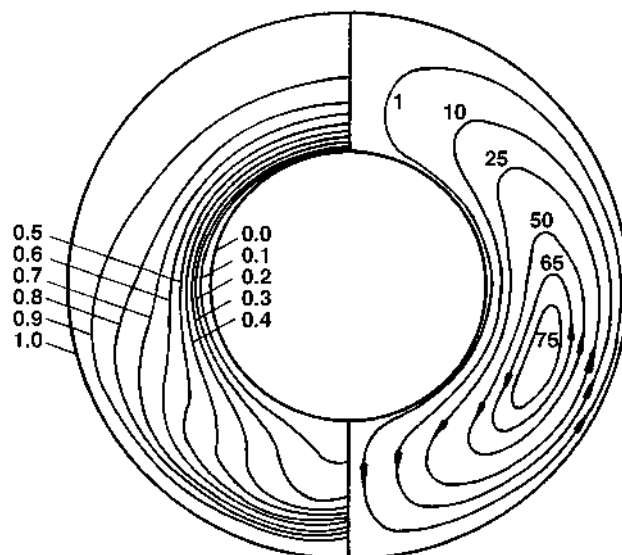


**Figure 3.**  
Isotherms and  
secondary flow ( $-10^4\psi$ )  
for  $\tilde{\mu} = 2$ ,  $\eta = 0.5$ ,  
 $Gr/Re^2 = 1$ ,  $Re = 50$ ;  
 $Pr = 10$

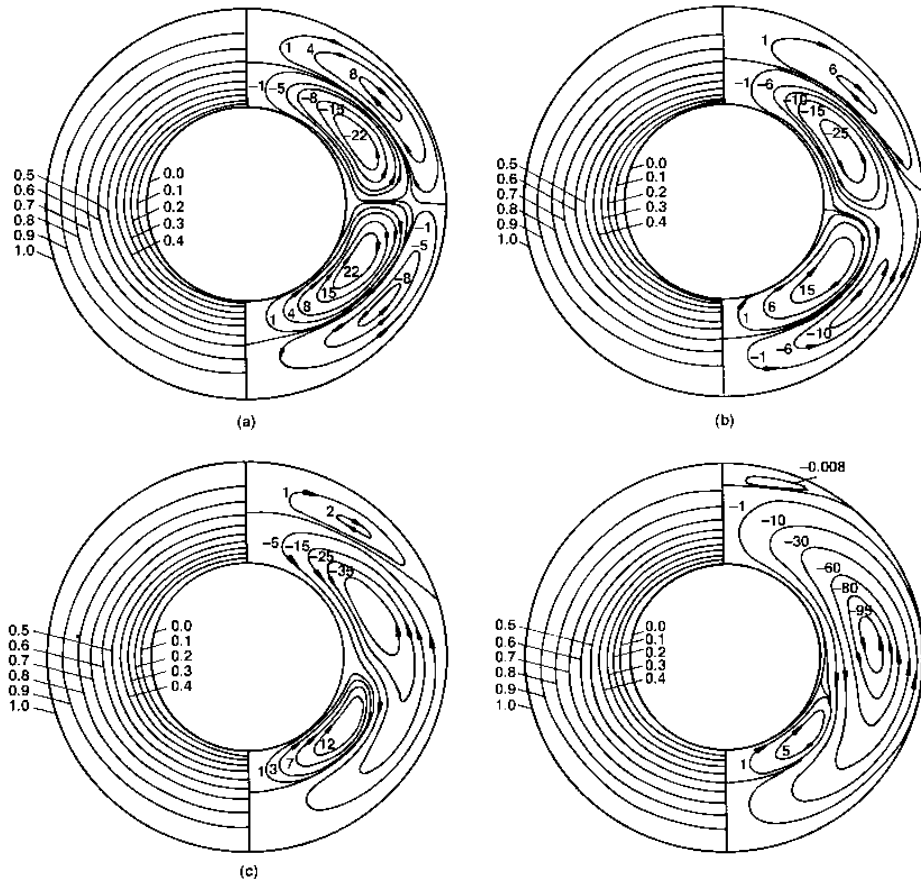


**Figure 4.**  
Isotherms and  
secondary flow ( $10^4\psi$ )  
for  $Re = 50$ ,  $\bar{\mu} = -1/3$ ,  
 $\eta = 0.5$ ,  $Pr = 1$ :  
(a)  $Gr/Re^2 = 0$ ;  
(b)  $Gr/Re^2 = 1/10$ ;  
(c)  $Gr/Re^2 = 1/3$ ;  
(d)  $Gr/Re^2 = 1$

the two counterclockwise eddies. This direction of circulation is preferred and encouraged by the gravitational field. As buoyancy forces increase through  $Gr/Re^2 = 1/3$  to 1 (Figure 4(c) and (d)), the counterclockwise eddies are totally merged and enhanced while the two clockwise eddies are very much reduced in size and strength. However, even for  $Gr/Re^2 = 1$ , the centrifugally driven eddies are not obscured, indicating that both the driving mechanisms still exist. These results are in good agreement with those of Dallman and Douglass (1980). For this set of flow parameters, the isotherms and angular velocity contours remain almost the same from their characteristic forced convection, concentric circular pattern (the isotherms are given in Figure 4). Additional insight into the effects of convective activity on the heat transfer in the annulus can be gained by the total heat transfer rate and the torque required to rotate the spheres or moment acting on the spheres. These will be of importance in thermal design application since for each net heat exchange rate, power (i.e. torque) needs to be supplied in order to keep the spheres in motion.

The total heat flux  $\Theta$  is found by integrating the gradient weighted by  $\sin \theta$  (because of the surface area effects) over the surface of the spheres and is given by:

$$\Theta = \frac{\Theta'}{kR_2(T_2 - T_1)} = 2\pi \int_{\theta=0}^{\pi} \sin \theta \left[ r^2 \frac{\partial T}{\partial r} \right]_{\eta,1} d\theta \quad (22)$$

The total rate of heat transfer for the condition is used to normalize  $\Theta'$ , where:

$$\Theta' = \frac{4\pi\eta}{(1-\eta)} [R_2 k (T_2 - T_1)].$$

In steady flows, the total heat transfer rate across each sphere must be the same, since dissipation is neglected. In the assumed axially symmetric flow, the mechanism for convection is observed to be only the stream function as seen in energy equation (3). Thus, the explanation of the behavior of  $\Theta \backslash \Theta_c$  as it depends on the flow parameters is related to that of  $\psi$ . Especially, the size of the convective energy terms (involving  $T$  and  $\psi$ ) is indicated by the product  $RePr$ . As shown in Figures 1 and 3, the magnitude of secondary circulation increases with  $Re$  and  $Pr$ . Hence, it is possible for  $\Theta \backslash \Theta_c$  to increase with increasing  $Re$  and  $Pr$ . This is shown in Figure 5 (solid lines).

The torque  $\tau$  required to rotate a sphere, is found by integrating the shear stress over the surface of the sphere to obtain:

$$\tau = \frac{\tau'}{\mu R_2^3 \omega_0} 2\pi \int_{\theta=0}^{\pi} \sin \theta \left[ r^4 \frac{\partial}{\partial r} \left\{ \frac{\Omega}{r^2} \right\} \right]_{\eta,1} d\theta \quad (23)$$

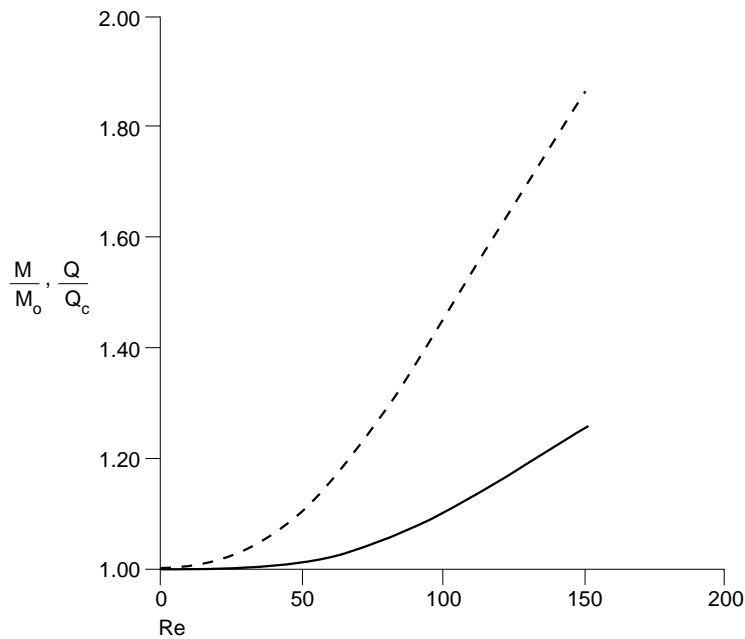


**Figure 5.**  
The effect of increasing  
 $Re$  on the total heat  
transfer (—) and the  
torque (---) for  $\bar{\mu} = 2$ ;  
 $\eta = 0.5$ ;  $Gr/Re^2 = 1$  and  
 $Pr = 1$

It is useful to non-dimensionalise the torque by its value for creeping flow,  $\tau_0$  given by:

$$\tau_0 = 8\pi\mu R_2^3 \frac{(\omega_2 - \omega_1)}{(1 - \eta^3)} \eta^3$$

giving 
$$\frac{\tau}{\tau_0} = \frac{(1 - \eta^3)\omega_0}{4\eta^3(\omega_2 - \omega_1)} \int_{\theta=0}^{\pi} \sin \theta \left[ r^4 \frac{\partial}{\partial r} \left\{ \frac{\Omega}{r^2} \right\} \right]_{\eta,1} d\theta \quad (24)$$

Like the total heat transfer rate, the magnitude of the torque required to rotate each sphere must be the same in steady state flow. The results for the dependence of the torque on  $Re$  is shown in Figure 5. It is observed that the general behavior of both  $\Theta \setminus \Theta_c$  and  $\tau/\tau_0$  is similar.

Lastly, the other limiting case of  $Gr/Re^2$ , i.e.  $Gr/Re^2$  large is studied. This is done by taking  $Gr = 1$  and  $Re = 0.5, 0.1, 0.05$  and  $0.01$ , i.e. for  $Gr/Re^2 = 4, 100, 4,000$ , and  $10,000$ . The other parameters are taken as  $Pr = 1, \eta = 0.5$  and  $\tilde{\mu} = -1/3$ . Figure 6 shows the secondary flow streamlines for this set of parameters. For large values of  $Gr/Re^2$ , even for  $\tilde{\mu} = -1/3$ , the annulus is spanned by single eddy only, which is generally observed in natural convection dominated flow only.

### 5. Conclusion

Parametric spline function approximation is used to study the steady combined convection in a rotating spherical annulus. The gravitational field acts parallel to the rotation axis and provides the driving force for buoyancy effects when the spheres are maintained at different temperatures. In the present approximation the first order derivatives of the non-linear terms in the governing equations are eliminated. This gives the advantage over usual finite difference scheme in which first order upwind differences will be applied to approximate the non-linear terms. The present approximation gives second order accuracy.

There are five dimensionless parameters governing the flow and heat transfer in the rotating annulus. The ratio of radii  $\eta = R_1/R_2$  is fixed as 0.5 throughout the calculations. The ratio of angular velocities of the spheres  $\tilde{\mu} = \omega_2/\omega_1$  as well as the other parameters  $Re, Gr, Pr$  affect the nature of the secondary flow and heat transfer rate. Positive values of  $\tilde{\mu}$  cause a single eddy pattern while the negative values result in double eddy patterns. The secondary flow and heat transfer rate increase with increasing  $Re$ . The Grashof number is an indicator of the effect of buoyancy forces and appears in the ratio  $Gr/Re^2$ . The forced convection case is given by  $Gr/Re^2 = 0$  and in this case  $\tilde{\mu} < 0$  causes the equatorial symmetry in secondary flow streamline pattern. Increasing the Prandtl number results in a slightly retarded secondary flow and causes locally larger temperature gradients. This results in larger total heat transfer rates. It is also observed that the torque required to rotate the spheres increases with increasing  $Re, Gr/Re^2, Pr$ .

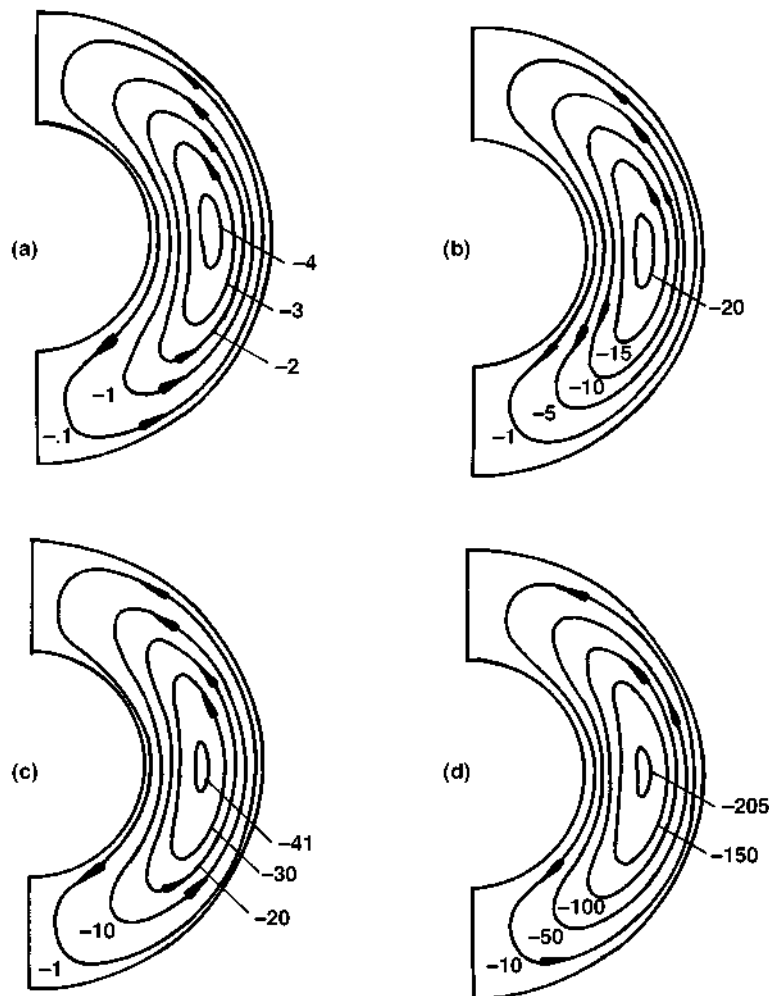


**Figure 6.**  
Secondary flow  
streamlines ( $10^4\psi$ ) for  
 $\bar{\mu} = -1/3$ ;  $\eta = 0.5$ ;  
 $Pr = 1$ ;  $Gr = 1$ ;  
(a)  $Re = 0.5$ ; (b)  $Re = 0.1$ ;  
(c)  $Re = 0.05$ ;  
(d)  $Re = 0.01$

### References

- Bestman, A. (1978), "Heat transfer in the biconical and concentric spherical viscometer", *J. Heat Transfer*, Vol. 100, pp. 750-2.
- Dallman, R.J. and Douglass, R.W. (1980), "Convection in a rotating spherical annulus with a uniform gravitational field", *Int. J. Heat Mass Transfer*, Vol. 23, pp. 1303-12.
- Douglass, R.W., Munson, B.R. and Shaughnessy, E.J. (1978), "Thermal convection in rotating spherical annuli - 2 stratified flows", *Int. J. Heat Mass Transfer*, Vol. 21, pp. 1555-64.
- Douglass, R.W., Munson, B.R. and Shaughnessy, E.J. (1979), "Small Reynolds convection in rotating spherical annuli", *Journal of Heat Transfer*, Vol. 101, pp. 427-33.
- Jain, M.K. and Aziz, T. (1981), "Spline function approximation for differential equations", *Comp. Meth. in Appl. Mech. and Eng.*, Vol. 26, pp. 129-43.
- Lauriat, G. and Altimir, I. (1985), "A new formulation of the SADI method for the prediction of natural convection flows in cavities", *Compt. Fluids*, Vol. 13, pp. 141-55.

---

**HFF**  
**8,6**

Maples, G., Dyer, D.F., Askin, K. and Maples, D. (1973), "Convective heat transfer from a rotating inner sphere to a stationary outer sphere", *Trans. ASME*, pp. 546-7.

Pedlosky, J. (1969), "Axially symmetric motion of a stratified rotating fluid in a spherical annulus of a narrow gap", *J. Fluid Mech.*, Vol. 36, part 2, pp. 401-15.

Raghavarao, C.V. and Srinivas, S.T.P.T. (1995a), "A numerical study of thermal convection in a rotating spherical annulus with radial gravitational field using parametric spline function approximation", *Proc. 9th Int. Conf. on Num. Meth. in Laminar and Turbulent Flow*, July, pp. 644-55.

**688**

---

Raghavarao, C.V. and Srinivas, S.T.P.T. (1995b), "A note on parametric spline function approximation", *Comp. Math. Appl.*, Vol. 29 No. 12, pp. 67-73.

Riley, T.A. and Mack, L.R. (1972), "Thermal effects on slow viscous flow between rotating concentric spheres", *Int. J. Non-linear Mech.*, Vol. 7, pp. 275-88.

Wang, P. (1987), "Spline method of fractional steps in numerical model of unsteady natural convection flow at high Rayleigh number", *Numer. Heat Transfer*, Vol. 11 No. 1, pp. 95-118.

Wang, P., Kahawita, R. and Nguyen, T.H. (1990), "Numerical computation of flow about a horizontal cylinder using splines", *Numer. Heat Transfer, Part A*, Vol. 17, pp. 191-215.